

D.C., 1966), Chap. 5.

<sup>26</sup>A. G. Cade, Phys. Rev. Letters **15**, 238 (1965).

<sup>27</sup>R. L. Douglass, Phys. Rev. Letters **13**, 791 (1964).

<sup>28</sup>In most cases where this correction is important,  $P_n^{-1}$ , while small, is large compared to the time required to accelerate the bare ion to a velocity near  $v_{eq}^{ion}$ , so that  $P_n(v) \exp[-\int_0^T P_n(v') dT']$  can be replaced by  $P_n(v_{eq}^{ion}) \times \exp[-P_n(v_{eq}^{ion})T]$  and we have  $\langle T \rangle \approx [P_n(v_{eq}^{ion})]^{-1}$ ,  $\langle X \rangle \approx v_{eq}^{ion} \langle T \rangle$ .

<sup>29</sup>The only exception is a single narrow region of field

and temperature near  $E = E_{c1}$  and  $T$  such that  $P_e(E_{c1}, T) \sim \tau_d^{-1}$ . This case can be treated by a straightforward generalization of Eq. (4.10).

<sup>30</sup>A. J. Dahm and T. M. Sanders, Jr., Phys. Rev. Letters **17**, 126 (1966).

<sup>31</sup>T. C. Padmore, Phys. Rev. Letters **26**, 63 (1971).

<sup>32</sup>K. W. Schwarz, Phys. Rev. **165**, 323 (1968).

<sup>33</sup>R. E. Little, Bull. Am. Phys. Soc. **16**, 639 (1971).

<sup>34</sup>R. L. Douglass, Phys. Rev. **165**, 323 (1968).

## Ultraviolet Emission Spectrum of Electron-Bombarded Superfluid Helium\*

M. Stockton, J. W. Keto, and W. A. Fitzsimmons

*University of Wisconsin, Madison, Wisconsin 53706*

(Received 23 June 1971)

The emission spectrum of electron-bombarded superfluid helium has been measured as a function of wavelength between 600 and 1100 Å. The spectrum is characterized by a very intense band of continuous emission peaking at approximately 800 Å, along with a series of less intense bands between the wavelengths of 600 and 710 Å. This continuum is interpreted in terms of the radiative dissociation of neutral helium molecules in the reaction  $A^1\Sigma_u^+ \rightarrow X^1\Sigma_g^+$ . The over-all intensity corresponds to about  $5 \times 10^{15}$  (photons/sec)/ $\mu\text{A}$  of 160-keV electron beam excitation. The uv fluorescence of electron-bombarded superfluid helium is by far the most intense emission of the excited liquid and may represent a useful source of uv light.

### I. INTRODUCTION

Considerable experimental effort has been directed toward the fast-particle bombardment of liquid helium as a method of studying the microscopic structure of simple liquids. The possible existence of identifiable neutral electronically excited states of the liquid is of particular interest since it is expected that such excitations could be used to probe the liquid structure. The experimental results presented in this paper indicate that the  $A^1\Sigma_u^+$  state of the neutral helium molecule is the neutral excitation that is most readily produced in electron-bombarded superfluid helium.

The scintillation of liquid helium in the vacuum ultraviolet due to  $\alpha$ -particle excitation was studied by Moss and Hereford almost a decade ago.<sup>1</sup> On the basis of an apparent inhibition of this scintillation below the  $\lambda$  temperature, these authors suggested the possible existence of excited atomic and perhaps even metastable states of the liquid. At about the same time, Jortner *et al.* provided additional evidence of neutral excitations in liquid helium by observing the enhanced emission of oxygen and nitrogen impurities in the liquid when subjected to  $\alpha$ -particle bombardment.<sup>2</sup> These authors proposed the existence of an efficient energy-transfer mechanism to the colloiddally suspended impurities. These suggestions have been supported by the observations of Surko and Reif which established

the existence of long lived but as yet unidentified neutral excitations in superfluid helium.<sup>3</sup> The question of identifying the nature of the electronic excitations in liquid helium has been very difficult due to a lack of sufficient intensity to allow spectroscopic measurements.

More recently, electron beams have been used to excite liquid helium. This experimental method has the advantage that the levels of particle bombardment can be substantially greater than what is attainable with a manageable radioactive source. In addition the transient behavior of the excitations produced in the liquid can be studied by pulsing the source of electrons. The use of electron beams has made possible the first direct spectroscopic identification of electronically excited atomic and molecular states in liquid helium.<sup>4-6</sup> The localized nature of the excitations is demonstrated by the vibrational and rotational structure of the observed helium molecular fluorescence.<sup>7</sup> These experiments have shown that large concentrations of both the atomic  $2^3S$  and molecular  $a^3\Sigma_u^+$  metastable states of helium are present in the excited liquid and they have shown in addition that the lowest bound  $A^1\Sigma_u^+$  state of  $\text{He}_2$  is populated at a rapid rate.<sup>4,6,8</sup> The dynamical properties of the atomic and molecular metastable states in liquid helium have been studied recently through the time dependence of the absorption and emission spectra; however, the present authors discuss this subject in a

future paper.<sup>9,10</sup>

The experimental measurements that are reported here result from an investigation of the uv emission of electron beam excited superfluid helium. The observed spectrum is characterized by a broad asymmetric peak near 800 Å plus a series of less intense bands between the wavelengths of 600 and 710 Å. It is of interest to note that simultaneous with the preliminary report of this work,<sup>6</sup> Surko *et al.* reported essentially the same spectrum even though the authors used a comparatively weak  $\beta$  emitter as a source of excitation.<sup>11</sup> Thus the uv spectrum of liquid helium appears to be independent of the source of electron excitation. We interpret the observed uv continuum in terms of the radiative dissociation of the  $A^1\Sigma_u^+$  state of the neutral helium molecule. Measurements of the absolute intensity indicate that the  $A^1\Sigma_u^+$  state is produced at the rate of approximately  $10^{17}/\text{sec}/\text{cm}^3$  with 1  $\mu\text{A}$  of 160-keV electrons stopped in the liquid. Since the preliminary report of this work, we have made a more extensive investigation of the series of bands that characterize the continuum between the wavelengths of 600 and approximately 710 Å. These bands are interpreted in terms of radiative dissociation that originates from a very high vibrational level of the  $A^1\Sigma_u^+$  state.<sup>12-15</sup> We suggest that the population of this vibrational level is caused by the production and subsequent resonant tunnelling of metastable  $2^1\text{S}$  helium atoms through the repulsive barrier which describes the  $\text{He}(2^1\text{S}) - \text{He}(1^1\text{S})$  molecular potential function at intermediate nuclear separations.<sup>16-19</sup>

## II. EXPERIMENTAL PROCEDURE

The basic experimental procedure consists of directing a beam of electrons into a sample of purified liquid helium and measuring the intensity of the resulting fluorescence as a function of wavelength.<sup>4,6,20</sup> The electrons, with nominal energy of 160 keV, are stopped in the liquid after passing through a thin metal foil that separates the liquid sample from the common vacuum of the electron accelerator and the liquid-helium cryostat. The investigation of the uv spectrum is complicated somewhat because the region of excitation (i. e., the small volume of approximately  $0.04 \text{ cm}^3$  in which the electrons are stopped) must be viewed directly without any intervening optical barriers such as windows or lenses. Furthermore, the sample must be pure liquid helium in order to avoid quenching of the uv fluorescence due to the presence of atmospheric gas impurities.

The measurements were carried out at temperatures below the  $\lambda$ -transition temperature of liquid helium in order to take advantage of the anomalously large thermal conductivity of superfluid helium which prevents the liquid from boiling. As has

been shown previously, and confirmed in this laboratory, under the present experimental conditions the energy dissipated by the incident electron beam does not cause the liquid to boil, and thus the physical observations are indeed characteristic of the liquid.<sup>4,6</sup>

The electron accelerator used throughout these experiments is shown schematically in Fig. 1. Electron beam currents between zero and several mA at energies up to 200 keV are available. The electrons, emitted by a hot tungsten filament, pass first through a negative self-biased grid which controls and regulates the beam current, are then focussed by the plate of the triode source, and are finally accelerated horizontally toward ground potential through a commercially available accelerating column. After acceleration, the beam passes between a set of horizontal and vertical deflection plates as well as through a focussing solenoid. These direct and focus the electrons through a 3-mm diam hole in a beam defining electrode that is located several in. in front of the liquid sample. A second set of electrostatic deflection plates is used to deflect the beam so as to miss the defining aperture; in this way the beam entering the sample may be pulsed on and off in less than  $10^{-8}$  sec with any desired duty cycle.<sup>10</sup>

After passing through the defining aperture, approximately half of the electrons are intercepted by a coarse copper screen with the remaining beam continuing toward the sample. The current collected by the screen is used to monitor the beam current throughout an experimental run; under normal conditions the fluctuations of the beam current are less than  $\pm 5\%$ . The electron current entering the sample is determined by measuring the current collected in a magnetically actuated Faraday cup that is positioned immediately before the liquid-helium Dewar. When energized the Faraday cup intercepts all of the beam that would otherwise be stopped in the sample.

As indicated in Fig. 2, the liquid sample is contained in a copper chamber that is located near the bottom of the helium cryostat. The copper walls thermally connect the sample to the surrounding liquid-helium bath. A thin (0.000125 in.) metal foil separates the sample from the common vacuum of the accelerator and the helium Dewar. The foil is a nonmagnetic cobalt-based alloy and it is soft soldered to the end of a  $\frac{5}{16}$ -in. -i. d. stainless-steel tube.<sup>21</sup> Since the range of 160-keV electrons in liquid helium is of the order of 3 mm, the foil mount must extend into the sample chamber such that the excitation volume is located immediately below the entrance slit of the uv spectrograph. The sample chamber and the uv spectrograph form a completely isolated vacuum system that is maintained at a pressure of  $10^{-6}$  Torr between experi-

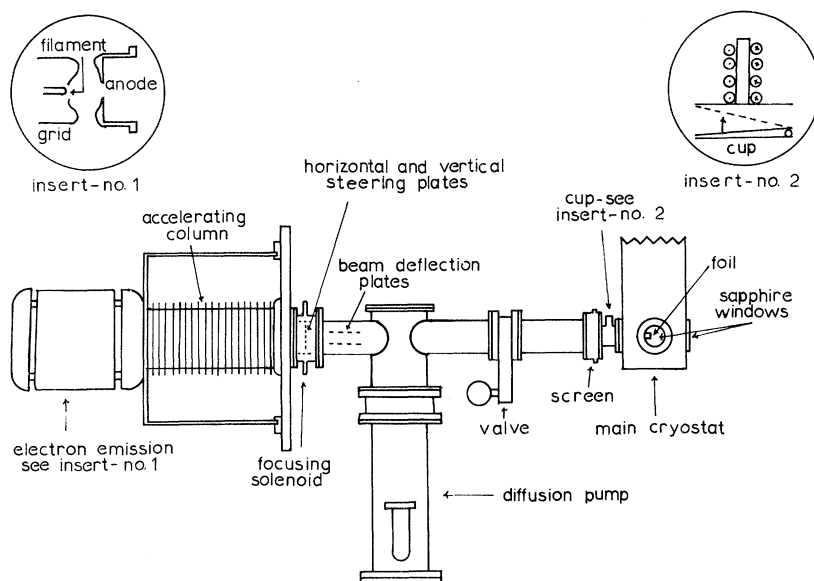


FIG. 1. Experimental apparatus: electron accelerator, beam tube, and lower portion of liquid-helium cryostat.

ments. Prior to each experiment, the spectrograph is filled with purified helium gas which is subsequently condensed into the liquid phase, filling the sample chamber. The helium gas is purified by passage through a liquid-nitrogen-cooled charcoal trap followed by a liquid-helium-cooled trap containing copper turnings.

The copper chamber, the helium tail of the Dewar, and the outer vacuum jacket are each provided with a set of three sapphire windows. The windows provide visual access to the excitation region in directions both parallel and perpendicular to the incident electron beam and are used during experiments which involve the visible and infrared spectroscopy of the liquid. Demountable flanges and connections are sealed with compressed indium metal O rings. The sapphire windows are epoxy bonded to stainless-steel window frames or, in some cases, sealed with indium O rings.

The temperature of the liquid sample is controlled by pumping on the cryogenic helium and regulating its vapor pressure. The lowest attainable temperature of approximately  $1.4^\circ\text{K}$  is determined by the available pumping capacity of roughly  $150\text{ ft}^3/\text{min}$  and the heat leaks of the present apparatus. Although the bath temperature is measured and regulated to within a few percent, the largest uncertainty in the sample temperature arises from the thermal boundary impedance between the liquid contained in the copper chamber and the surrounding helium bath. At a nominal temperature of  $1.4^\circ\text{K}$  and with  $1\ \mu\text{A}$  of 160-keV electron beam stopped in the sample, the measured temperature of the sample is approximately  $0.06^\circ\text{K}$  greater than that of the bath. As will be discussed later, this thermal impedance restricts the upper limit on

beam current to roughly  $8\ \mu\text{A}$  before the sample is driven above the  $\lambda$ -transition temperature and the liquid begins to boil.

The vacuum uv spectrograph shown schematically in Fig. 2 was designed and built in this laboratory to be compatible with the existing helium cryostat and electron accelerator. The design objective was to have fixed entrance and exit slits and to

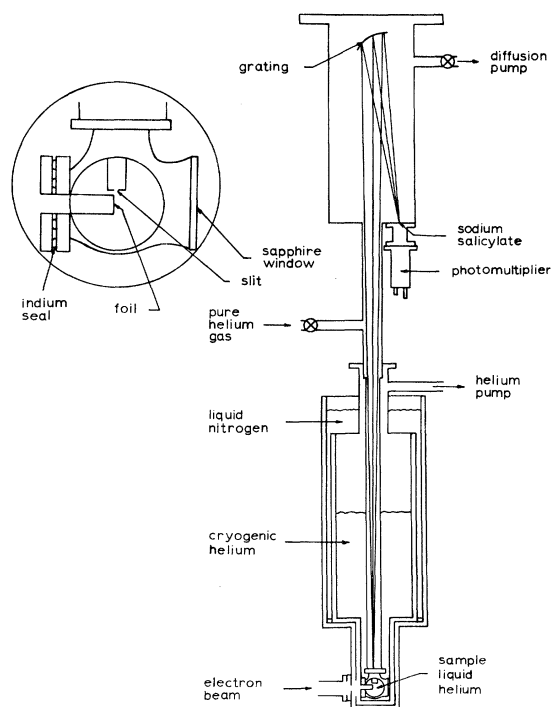


FIG. 2. Experimental apparatus: liquid-helium cryostat, sample chamber, and vacuum uv spectrograph.

have the wavelength scanned by a simple rotation of the concave grating without a substantial defocusing of the instrument. The spectrograph may be described by starting with the condition for first-order constructive interference from a grating:

$$\lambda = d(\sin\alpha + \sin\beta), \quad (1)$$

where  $\alpha$  and  $\beta$  are the angles of incidence and defraction, respectively, and are measured relative to the grating normal,  $d$  is the distance between the rulings on the grating, and  $\lambda$  is the wavelength of the light. For a concave grating having a radius of curvature  $r$ , the object distance  $s$ , and the image distance  $r'$  are related to  $\alpha$  and  $\beta$  through<sup>22</sup>

$$r' = \frac{r \cos^2 \beta}{\cos \alpha [1 - (r/s) \cos \alpha] + \cos^2 \beta}. \quad (2)$$

Despite the use of fixed slits, the near normal incidence mount allows both the angles  $\alpha$  and  $\beta$  to remain simultaneously small for reasonably large variations of the wavelength. In addition, with the proper choice of object distance, the image distance, as given by Eq. (2), becomes roughly independent of these angles. This situation is realized if  $s = 2r$  and  $r'$  becomes

$$r' = \frac{2}{3} r (1 + \frac{1}{3} \beta^2). \quad (3)$$

The expansion has been carried out through second order in the small angles with the result being independent of the angle of incidence. Our instrument is fitted with a gold replica grating having 1440 grooves/mm and a 1-m radius of curvature.<sup>23</sup> The object distance is 2 m and the image distance is 0.666 m. The exact value of the image distance may be adjusted slightly to improve the focal properties of the instrument over the desired wavelength region. In our case  $\beta = \alpha - 6.2^\circ$  where  $6.2^\circ$

is twice the blaze angle of the grating. Over the wavelength interval of 500 to 1700 Å the angle  $\beta$  varies between approximately  $-1^\circ$  and  $+4^\circ$  and the image distance varies less than  $\pm 1$  mm out of a total of 666 mm.

Two exit slits were installed symmetrically on either side of the incident direction in order that the spectrograph could be aligned after being connected to the helium Dewar. Alignment is achieved by adjusting the relative position of the entrance slit until its zeroth order image could be displaced from the incident direction into each exit slit by equal angular rotations of the grating.

The optical signal is detected by observing the secondary fluorescence from a window which is coated with sodium salicylate and which forms the vacuum seal directly behind the exit slit.<sup>24</sup> The secondary fluorescence signal is detected with a EMI 6256 photomultiplier, amplified by a Keithley 610B electrometer having a 1-sec time constant, and plotted on a strip-chart recorder.

The spectrograph was tested by observing the spectrum from a discharge tube similar to that used by Huffman *et al.* in their investigation of the uv emission of gaseous helium.<sup>25</sup> A small amount of neon was added to the discharge and the 736- and 744-Å resonance lines of neon were used to calibrate the instrument. With entrance and exit slits of 240 and 80  $\mu$ , respectively, the observed spectrum, shown in Fig. 3, is consistent with the expected resolution of approximately 1 Å.

### III. EXPERIMENTAL RESULTS

The uv emission spectrum of electron excited superfluid helium is shown in Fig. 4. The instrumental resolution is approximately 1 Å. The solid curves numbered 1 and 2 are tracings of the original data that were taken with sample temperatures

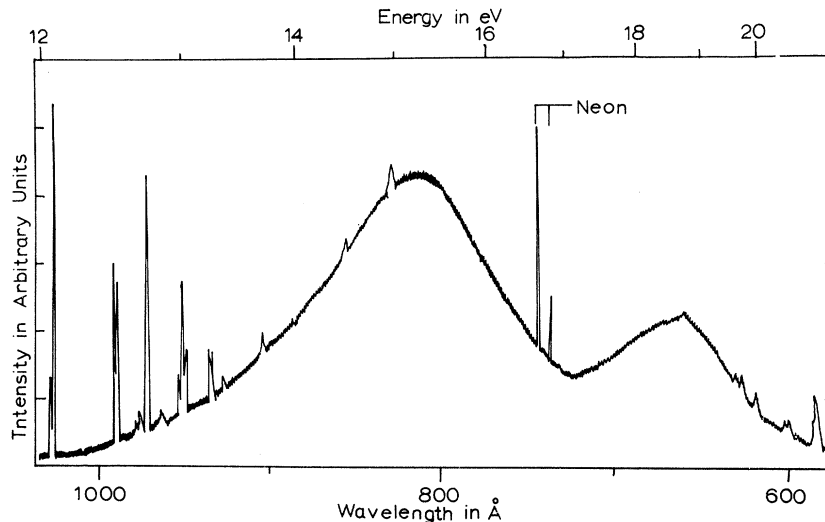


FIG. 3. Ultraviolet emission spectrum of a high-pressure helium discharge lamp. The lines labeled neon are the 736- and 744-Å resonance lines of the neon impurity in the lamp, and they indicate the 1-Å resolution of the spectrograph used throughout these experiments.

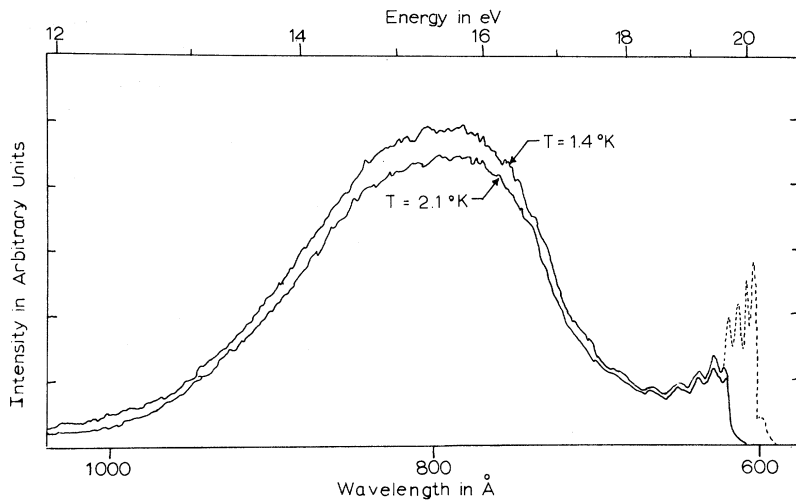


FIG. 4. Ultraviolet emission spectrum of electron-bombarded superfluid helium. Solid curves are for  $1 \mu\text{A}$  of electron excitation at temperatures of 2.1 and 1.4 °K, respectively. The dotted curve represents the shorter-wavelength bands which are absorbed within the first several mm of ground-state liquid.

of 2.1 and 1.4 °K, respectively. The shape of the continuum does not exhibit a significant variation with temperature, although the intensity increases by roughly 10% as the temperature is reduced from 2.1 to 1.4 °K. Throughout most of the experiments the free surface of the liquid sample was between 1 and 15 cm above the entrance slit to the spectrograph. Despite this variation of liquid level no change in the intensity or shape of the continuum was noted. Thus the liquid is transparent to wavelengths greater than 620 Å. Surko *et al.* have pointed out that the first few mm of the unexcited liquid absorb light that is emitted between the wavelengths of 600 and 620 Å.<sup>11</sup> We have observed a similar result by reducing the liquid level in the sample chamber until it essentially divided the incident electron beam. The self-absorbed portion of the continuum is indicated by the dotted lines in Fig. 4 and is shown with greater detail in Fig. 5. The absorbed bands are evidently a continuation of the structure that is apparent at longer wavelengths. We were unable to obtain reliable measurements of the self-absorption as a function of level height because the transverse dimensions of the electron beam are of the same order as the 2 or 3 mm characteristic absorption path length. However, the series of bands shown in Fig. 5 are due to the fluorescence of the liquid since no spectra could be recorded when the liquid level was positioned below the incident electron beam.

Perhaps the most important result of these experiments is the unexpected intensity of the uv light emitted by electron excited superfluid helium. We estimate that the integrated flux emitted into  $4\pi\text{sr}$  from an excitation volume of  $0.04 \text{ cm}^3$  corresponds to  $5 \times 10^{15}$  (photons/sec)/ $\mu\text{A}$  of 160-keV electron beam excitation. This corresponds to a measured flux exiting the spectrometer of  $10^7$  (photons/sec) per Å bandwidth at the continuum peak of 800

Å. The intensity of this source was determined by first measuring the photoconversion efficiency of the combined sodium salicylate film, collecting lens, and EMI 6256S photomultiplier system using the 2540-Å resonance emission of a mercury lamp as a source of uv. It was assumed that the conversion efficiency of the sodium salicylate is independent of wavelength between 600 to 2540 Å.<sup>24</sup> The intensity of the 2540-Å mercury line was measured by comparison with a commercially available sec-

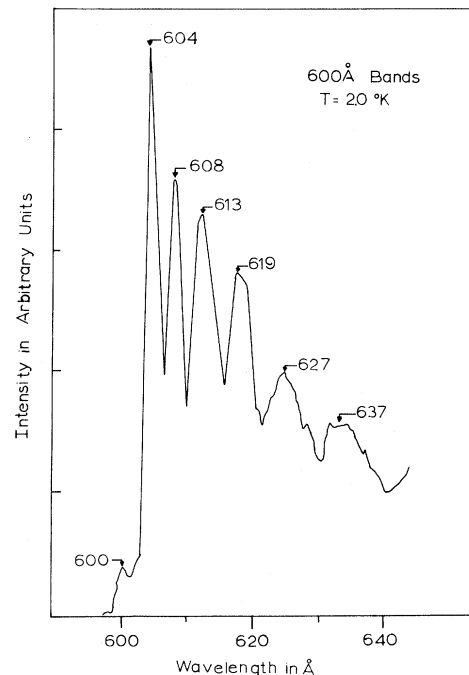


FIG. 5. 600-Å bands emitted by electron-bombarded superfluid helium. Spectrum observed by locating the free surface of the liquid sample at the position of the incident electron beam.

ondary standard lamp that had been masked with a  $(3600 \pm 400)\text{-\AA}$  band pass filter. The relative quantum efficiency of the photomultiplier as a function of wavelength was presumed to be given by the manufacturer's specifications. The absolute intensity of the uv light exiting the spectrometer in zeroth order (i. e., using the grating as a mirror) was determined, and then referred back to the original source by correcting for solid angle factors and by making the conservative assumption that the reflectivity of the gold replica grating was 100%. The uncertainty in the final result of  $5 \times 10^{15}$  photons/sec probably does not exceed a factor of 2. A similar result for the source intensity was obtained by observing the secondary fluorescence emitted by a sodium salicylate film that was placed in the liquid sample at a distance of approximately 3 cm from the excitation region.<sup>6</sup> The over-all intensity of the uv continuum indicates that approximately 10% of the beam energy is converted into uv light.

The intensity of the uv continuum is observed to increase linearly with beam current at all wavelengths, to within an estimated  $\pm 5\%$  experimental uncertainty, for beam currents between 0.05 and 8.0  $\mu\text{A}$  at a nominal electron energy of 160 keV. Electron beam currents of the order and greater than 8  $\mu\text{A}$  resulted in the boiling of the liquid sample and a sharp decrease in the uv intensity. The upper limit on beam current is due to the thermal impedance or Kapitza effect that is associated with the conduction of heat across copper-liquid-helium interfaces.<sup>26</sup> With the present copper sample chamber the measured sample-to-bath temperature difference at low beam currents is approximately 0.06  $^\circ\text{K}/\text{mA}$  of 160-keV electron beam with a bath temperature of 1.4  $^\circ\text{K}$ . Because of the limited pumping capacity, the bath temperature rises at the higher beam currents and exceeds the 2.18  $^\circ\text{K}$   $\lambda$ -transition temperature of liquid helium and begins to boil at about 8  $\mu\text{A}$  of beam.

The uv intensity varied linearly with beam energy for accelerating potentials between 45 and 200 keV. The light output was zero for electron energies less than about 40 keV. This is to be expected since, at this energy, the range of electrons in high- $Z$  materials is of the order of the thickness of the foil.<sup>27</sup> However, with electron energies in the neighborhood of 160 keV, only several keV is lost to the foil.

Small quantities of neon were added to the liquid sample in order to investigate the effects of impurity atoms on the uv continuum. A molar concentration of no more than 0.01% neon in the liquid helium resulted in a substantial decrease in the intensity of the uv continuum. In addition the uv intensity was, in contrast to the emission of a pure sample, strongly dependent upon the temperature; increasing by about a factor of 10 as the tempera-

ture was reduced from 2.1 to 1.4  $^\circ\text{K}$ . Similar results have been reported by Surko *et al.* with the addition of nitrogen as an impurity and one may conclude that the full uv intensity will not be obtained unless the sample is carefully purified.<sup>11</sup> A detailed investigation of this quenching phenomenon is in progress and the results will be reported later.

#### IV. DISCUSSION

The prominent feature of the uv continuum of electron excited superfluid helium may be interpreted in terms of the radiative dissociation of the  $A^1\Sigma_u^+$  state of the neutral helium molecule. The dissociative reaction  $A^1\Sigma_u^+ - X^1\Sigma_g^+ + h\nu$  is known to be the source of the 825  $\text{\AA}$  band which, as shown by Fig. 3, characterizes the spectrum of a high-pressure helium discharge. The apparent broadening and shift of this feature toward shorter wavelengths suggests that the first several vibrational levels of the  $A^1\Sigma_u^+$  state are being populated in the liquid and are contributing to the observed continuum. This interpretation is supported by the previously reported infrared emission spectrum of electron-excited liquid helium which shows that at least the first four vibrational levels of the  $A^1\Sigma_u^+$  state are being populated.<sup>4</sup> However, it must be mentioned that when, under similar circumstances, the infrared radiative population of the  $A^1\Sigma_u^+$  state is approximately  $10^{13}/\text{sec}$ , the uv emission corresponds to a depopulating rate of  $5 \times 10^{15}/\text{sec}$ . Thus the principal mechanism for the formation of the  $A^1\Sigma_u^+$  state of  $\text{He}_2$  in the electron-excited liquid remains to be identified.

The series of bands between 600 and 710  $\text{\AA}$  shown in Figs. 4 and 5 is very similar to the so-called 600- $\text{\AA}$  bands that appear in the spectrum of an uncondensed helium discharge.<sup>28</sup> In Table I the posi-

TABLE I. Locations of the maxima for the 600- $\text{\AA}$  bands of  $\text{He}_2$  as they appear in the liquid spectrum, in the spectrum of a gaseous discharge (Ref. 12), and as predicted theoretically (Ref. 15).

$\lambda(\text{\AA})$ —Liquid	$\lambda(\text{\AA})$ —Gas	$\lambda(\text{\AA})$ —Theory
	600.07	600.0
(600)	600.06	600.6
	602.3	602.3
604	605.0	604.8
608	608.4	608.3
613	613.0	613.0
619	619.0	618.5
627	627	626
636	636	635
648	648	646
665	662	659
686	685	676
707	708	696

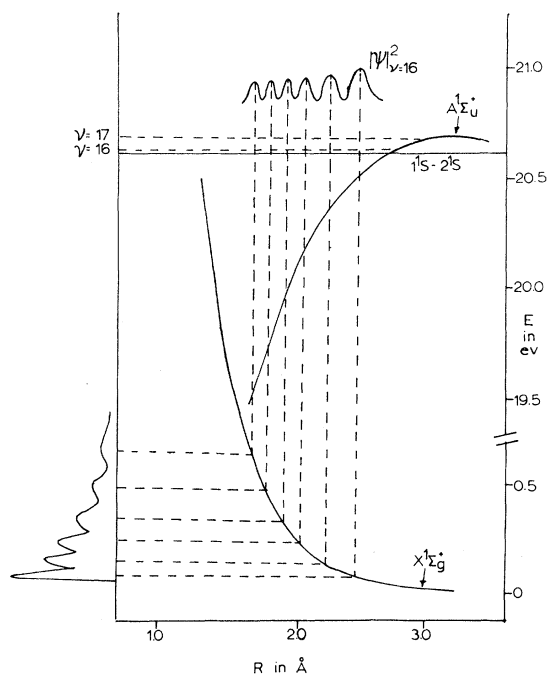


FIG. 6. Graphical representation of the qualitative features of emission from the second highest ( $\nu=16$ ) quasibound vibrational level of the  $A^1\Sigma_u^+$  state. The  $\nu=16$  level is estimated to be  $1.2 \times 10^{-2}$  eV above the He( $1^1S$ )-He( $2^1S$ ) separated atom limit (see Ref. 15).

tions of the emission maxima of the liquid-helium spectrum are compared to the previously measured and theoretically predicted positions of the 600-Å bands of a helium discharge.<sup>12,15</sup> The bands that are absent from the liquid spectrum, if in fact they are emitted, would be expected to be absorbed by the helium vapor that fills the spectrograph. The absorption of helium vapor in this wavelength region has been studied by Tanaka and Yoshino and they suggest the transition  $X^1\Sigma_g^+ \rightarrow A^1\Sigma_u^+$  to account for their results, where the  $X^1\Sigma_g^+$  state is temporarily formed at large internuclear separations during collisions between ground-state atoms.<sup>18</sup> This mechanism would be consistent with the additional absorption of the ground-state liquid shown in Fig. 4 since the formation of temporary  $X^1\Sigma_g^+$  molecules depends on the square of the ground-state atom density.

The theoretical interpretation of the 600-Å bands of helium is closely related to the details of both the  $A^1\Sigma_u^+$  and  $X^1\Sigma_g^+$  molecular potential curves. In particular the first several peaks in the spectrum of an uncondensed helium discharge imply the existence of a repulsive barrier in the  $A^1\Sigma_u^+$  molecular potential curve since the energies involved are slightly greater than the He( $1^1S$ )-He( $2^1S$ ) separated atom energy. The qualitative features of both the  $A^1\Sigma_u^+$  and  $X^1\Sigma_g^+$  potential curves are shown in

Fig. 6. The location and height of the repulsive barrier in the  $A^1\Sigma_u^+$  potential curve has been subject to considerable theoretical investigation. The most recent analysis indicates a barrier height of 0.049 eV located at an internuclear separation of 3.2 Å.<sup>15</sup> Mies and Smith suggest that the 600-Å bands of a helium discharge result from collisions between He( $1^1S$ ) and He( $2^1S$ ) atoms that have kinetic energy sufficient to pass over the repulsive barrier with the subsequent radiative dissociation originating from continuum states of the  $A^1\Sigma_u^+$  molecule.<sup>13</sup> However, since the barrier maximum corresponds to a temperature of approximately 575 °K, one would not expect this mechanism to account for the intensity of the bands that appear in the liquid spectrum. On the other hand, Sando has interpreted the 600-Å bands of the helium discharge in terms of the  $\nu=16$  and  $\nu=17$  quasibound vibrational levels of the  $A^1\Sigma_u^+$  state.<sup>15</sup> According to this analysis, dissociation originating from the  $\nu=16$  levels accounts for all but the shortest wavelength band that is emitted. These two vibrational levels, indicated by the dashed lines in Fig. 6, have energies estimated to be  $1.2 \times 10^{-2}$  and  $5 \times 10^{-2}$  eV, respectively, above the separated atom limit.

The correspondence between the bands of the liquid spectrum to those emitted by an uncondensed helium discharge strongly suggest a similar origin. Since the continuum states of the  $A^1\Sigma_u^+$  molecule can be ruled out, one must conclude that the bands of the liquid spectrum result from the rapid production of  $A^1\Sigma_u^+$  neutral helium molecules in the near zero energy  $\nu=16$  vibrational level. Since the short-wavelength bands account for approximately 10% of the over-all emission, the production rate of these particular molecules must be of the order of  $5 \times 10^{14}$ /sec with 1  $\mu A$  of 160-keV electron beam excitation. One is then left in the rather puzzling situation of trying to account for the rapid and selective population of one high-lying vibrational level of the  $A^1\Sigma_u^+$  state. A possible resolution of this question is suggested by the results of our recent investigation of the infrared optical absorption spectrum of electron excited superfluid helium. These experiments have shown that metastable  $a^3\Sigma_u^+$  helium molecules and metastable He( $2^3S$ ) atoms are produced at the rates of approximately  $10^{15}$ /sec and  $10^{14}$ /sec, respectively, when the production rate of the  $A^1\Sigma_u^+$  state corresponds to  $5 \times 10^{15}$ /sec. It therefore seems reasonable to presume a corresponding production rate for the metastable He( $2^1S$ ) atom. Noting the near resonance between the lowest quasibound vibrational level of the  $A^1\Sigma_u^+$  state and the He( $2^1S$ )-He( $2^1S$ ) separated atom energy, we suggest that this particular vibrational level is populated by the resonant tunnelling of He( $2^1S$ ) atoms through the repulsive potential barrier which separates the metastable state from the surrounding ground-state

atoms of the liquid.

The major features of the uv emission of liquid helium can be interpreted in terms of the radiative dissociation of the  $A^1\Sigma_u^+$  state of  $\text{He}_2$ . On the other hand, Surko *et al.* have noted a substantial distortion of the 800-Å peak along with an apparent quenching of the 600-Å bands with the addition of small quantities of nitrogen to the liquid helium.<sup>11</sup> The resulting spectrum appears to be a composite of two peaks, one near 825 Å and the other at approximately 755 Å. These authors note that the 825-Å feature would correspond to the ( $v=0$ )  $A^1\Sigma_u^+ \rightarrow X^1\Sigma_g^+$  transition, and they suggest that the 755-Å peak might correspond to the parity forbidden  $B^1\Pi_g \rightarrow X^1\Sigma_g^+$  transition if one allowed for a possible shift of about 25 Å toward shorter wavelengths. In addition, these authors observed that the distortion of the spectrum at the shorter wavelengths increased with increasing impurity concentration, and they suggest that this effect is consistent with the expected greater radiative lifetime of the  $B^1\Pi_g$  state which would make this state relatively more susceptible to quenching by the impurities. We would like to point out, however, that there is a substantially different and equally plausible explanation for these observations. The suggestion that the major feature of the continuum is a composite of two peaks near 800 Å is consistent with the analysis of Smith and Meriwether which shows that such an intensity distribution would be expected if there was a significant population of the  $v=1$  vibrational level of the  $A^1\Sigma_u^+$  state.<sup>29</sup> Furthermore, the increased distortion of the continuum with increasing impurity concentration could correspond to the quenching of the 600-Å bands which, as we have suggested, results

from the relatively slow tunnelling of  $2^1S$  metastable helium atoms. Thus, in this interpretation, it is the metastable  $2^1S$  state that is preferentially quenched by the impurities. It is evident, however, that a satisfactory interpretation of the impurity quenching phenomenon, as well as the details of the 800-Å peak, can not be made on the basis of the presently available data.

## V. SUMMARY

The continuous emission spectrum of electron-bombarded superfluid helium has been measured between the wavelengths of 600 and 1100 Å. The spectrum is characterized by a very intense continuum peaking at approximately 800 Å, with a series of less intense bands between the wavelengths of 600 and 710 Å. We interpret the observed spectrum in terms of the radiative dissociation of neutral helium molecules in the reaction  $A^1\Sigma_u^+ \rightarrow X^1\Sigma_g^+$ . Absolute measurements of the intensity show that the  $A^1\Sigma_u^+$  state of  $\text{He}_2$  is produced in the liquid at a rate of approximately  $5 \times 10^{15}$ /sec with  $1 \mu\text{A}$  of 160-keV electron excitation. These results suggest that the electron excitation of liquid helium may be a useful source of ultraviolet light. Our measurements indicate that the short-wavelength bands of the uv continuum are due to the rapid population of the  $v=16$  or lowest quasibound vibrational level of the  $A^1\Sigma_u^+$  helium molecule. It is suggested that the selective population of this vibrational level is caused by the production and subsequent resonant tunnelling of metastable  $2^1S$  helium atoms through the repulsive barrier that describes  $\text{He}(1^1S)\text{-He}(2^1S)$  interaction potential at intermediate nuclear separations.

\*Work supported in part by the National Science Foundation.

<sup>1</sup>Frank E. Moss and Frank L. Hereford, Phys. Rev. Letters **11**, 63 (1963).

<sup>2</sup>J. Jortner, L. Meyer, S. A. Rice, and E. G. Wilson, Phys. Rev. Letters **12**, 415 (1964).

<sup>3</sup>C. M. Surko and F. Reif, Phys. Rev. **175**, 229 (1968).

<sup>4</sup>W. S. Dennis, E. Durbin, Jr., W. A. Fitzsimmons, O. Heybey, and G. K. Walters, Phys. Rev. Letters **23**, 1083 (1969).

<sup>5</sup>M. Stockton and W. A. Fitzsimmons, Bull. Am. Phys. Soc. **15**, 247 (1970).

<sup>6</sup>M. Stockton, J. W. Keto, and W. A. Fitzsimmons, Phys. Rev. Letters **24**, 654 (1970).

<sup>7</sup>W. A. Fitzsimmons, J. W. Keto, M. Stockton, and L. J. Smith, Bull. Am. Phys. Soc. **15**, 57 (1970).

<sup>8</sup>J. C. Hill, O. Heybey, and G. K. Walters, Phys. Rev. Letters **26**, 1213 (1971).

<sup>9</sup>For a preliminary report see J. W. Keto and W. A. Fitzsimmons, Bull. Am. Phys. Soc. **15**, 247 (1970).

<sup>10</sup>J. W. Keto, M. Stockton, and W. A. Fitzsimmons (unpublished).

<sup>11</sup>C. M. Surko, R. E. Packard, G. J. Dick, and F. Reif, Phys. Rev. Letters **24**, 657 (1970).

<sup>12</sup>Y. Tanaka and K. Yoshino, J. Chem. Phys. **39**, 3081 (1963).

<sup>13</sup>Frederick H. Mies and Allen Laslett Smith, J. Chem. Phys. **45**, 994 (1966).

<sup>14</sup>A. L. Smith, J. Chem. Phys. **47**, 1561 (1967); **49**, 4813 (1968); **49**, 4817 (1968).

<sup>15</sup>K. M. Sando, in Proceedings of the Sixth International Conference on Electronic and Atomic Collisions, 1969, p. 894 (unpublished).

<sup>16</sup>R. A. Buckingham and A. Dalgarno, Proc. Roy. Soc. (London) **A213**, 327 (1952).

<sup>17</sup>D. R. Scott, E. M. Greenawalt, J. C. Browne, and F. A. Matsen, J. Chem. Phys. **44**, 2981 (1966).

<sup>18</sup>Y. Tanaka and K. Yoshino, J. Chem. Phys. **50**, 3087 (1969).

<sup>19</sup>K. M. Sando and A. Dalgarno, Mol. Phys. **20**, 103 (1971).

<sup>20</sup>W. S. Dennis, Ph.D. thesis (Rice University, 1969) (unpublished).

<sup>21</sup>HAVAR foil, manufactured by the Hamilton Watch Company, Lancaster, Pa.

<sup>22</sup>Ralph A. Sawyer, *Experimental Spectroscopy* (Dover, New York, 1963).

<sup>23</sup>Grating manufactured by Bausch and Lomb, Rochester,



New York.

<sup>24</sup>J. Samson, *Techniques of Vacuum Ultraviolet Spectroscopy* (Wiley, New York, 1967).

<sup>25</sup>R. E. Huffman, Y. Tanaka, and J. C. Larrabee, *Appl. Opt.* **2**, 617 (1963).

<sup>26</sup>J. Wilks, *The Properties of Liquid and Solid Helium* (Oxford U.P., London, 1967).

<sup>27</sup>Pierre Marmier and Eric Sheldon, *Physics of Nuclei*

and Particles (Academic, New York, 1969), Vol. I.

<sup>28</sup>The appearance of these bands depends upon the discharge conditions, and, as shown in Fig. 3, they do not appear in a condensed helium discharge. See, for example, Y. Tanaka, A. S. Jursa, and F. J. Le Blanc, *J. Opt. Soc. Am.* **48**, 304 (1958).

<sup>29</sup>Allan Laslett Smith and John W. Meriwether, Jr., *J. Chem. Phys.* **42**, 2984 (1965).

PHYSICAL REVIEW A

VOLUME 5, NUMBER 1

JANUARY 1972

## Absence of an Ehrenfest Phase Transition in a Hard-Core Lattice Gas?

R. M. Nisbet\* and I. E. Farquhar

*Department of Theoretical Physics, University of St. Andrews, St. Andrews, Scotland*

(Received 25 March 1971)

We report some numerical results for a lattice gas of hard-core molecules on the plane square lattice, occupancy of first, second, and fourth nearest neighbors to an occupied site being forbidden (1-2-4 model). Periodic lattices of even width up to 14 sites have been studied by the matrix method; the results indicate that any transition occurs at an activity  $z_t = 3.315 \pm 0.005$ . However, there is evidence that the transition is *not* first order; indeed it is likely that no Ehrenfest phase transition (EPT) occurs in the model.

### INTRODUCTION

Many workers have studied two-dimensional lattice systems<sup>1,2</sup> of molecules with extended hard cores and the results leave little room for doubt that an order-disorder transition is present in all such models. However, much of this work is motivated by a search for suitable models to describe freezing; the principal point of interest in this context is the presence or absence of a *first-order* Ehrenfest phase transition (EPT), neither possibility being, to the best of our understanding, inconsistent with the well-established order-disorder transition. Orband and Bellemans<sup>1</sup> summarized the results of various treatments of such models on both square and triangular lattices where calling, respectively,  $A, B, C, \dots$  the cases of exclusion up to 1st, 2nd, 3rd,  $\dots$  nearest-neighbor sites, they gave evidence for the behavior indicated in Table I.

They then suggested that the irregularity of the results for the square lattice was "probably due to the residual degrees of freedom persisting at close packing for cases  $B, D$ , and  $E$ , which allow adjacent rows of molecules to slide freely with respect to each other," unlike the triangular lattice where the close-packed configurations are well defined in all cases studied. On both lattices (excluding case  $A$  where the hard core may be too small) it is evident that in each case *the predicted EPT is first order when the close-packed configuration is well defined*. With the intention of testing this idea we studied the 1-2-4 model where the close-packed configuration is well defined and thus a first-order EPT should be ex-

pected. Preliminary results indeed indicated this first-order EPT but more detailed work, stimulated by recent conjectures<sup>3,4</sup> that systems with purely repulsive forces have no EPT, predicts no first-order EPT for the model.

### MATRIX METHOD

Periodic lattices of infinite length and of even width  $M$  up to 14 sites were studied by the matrix method.<sup>1</sup> A matrix  $B(z)$  is constructed, thermodynamic quantities deriving from the eigenvalue of maximum modulus (necessarily real and positive)  $\lambda_1$  and its derivatives. Denoting by  $\{\lambda_i\}$ ,  $\{x_i\}$ ,  $\{y_i\}$  the sets of eigenvalues and corresponding right and left eigenvectors of  $B$ , and by  $B'$  and  $B''$ , respectively, the matrices with  $(i, j)$ th elements  $dB_{ij}/dz$  and  $d^2B_{ij}/dz^2$ , we find from arguments similar to those of Wilkinson<sup>5</sup> that

$$\frac{d\lambda_1}{dz} = \frac{(y_1, B'x_1)}{(y_1, x_1)}$$

and

$$\frac{d^2\lambda_1}{dz^2} = \frac{1}{(y_1, x_1)} \left( (y_1, B''x_1) + 2 \sum_{j \neq 1} \frac{(y_j, B'x_1)(y_1, B'x_j)}{(\lambda_1 - \lambda_j)(y_j, x_j)} \right),$$

*provided  $B$  is not defective* (i.e., provided  $B$  possesses a complete set of right and left eigenvectors). This is not the case with the matrices of the 1-2-4 model where, even after symmetry reduction, we obtained  $n \times n$  matrices of rank  $r$  but with a zero eigenvalue of multiplicity  $p$  ( $p \neq n - r$ ). The difficulty may be overcome by deflating the matrix